Eur Biophys J (1989) 17: 131–136

European Biophysics Journal

Time-resolved refractive index change during the bacteriorhodopsin photocycle

N. V. Tkachenko, V. V. Savransky, and A. Yu. Sharonov

General Physics Institute, Vavilov st. 38, SU-117942 Moscow, USSR

Received December 14, 1988/Accepted January 24, 1989

Abstract. Kinetic refractive index spectroscopy has been applied to the study of the bacteriorhodopsin photocycle. A fully hydrated purple membrane film was examined in the temperature range from 10° to 40 °C using 532 nm excitation (doubled Nd YAG laser) and 633 nm (He-Ne laser) testing beam. Multi-exponential fitting of the data revealed five processes. Four of them are well known from kinetic optical absorption studies. The fifth process has only recently been observed in optical absorption experiments where it has a relatively small amplitude. In our refractive index experiments it has an amplitude of up to 30% of the full signal amplitude. It is characterized by an Arrhenius temperature dependence with an activation enthalpy of 40 ± 5 kJ/mol and a decay time of about 0.8 ms at 20 °C.

Key words: Bacteriorhodopsin, purple membrane, refractive index, photocycle, kinetic spectroscopy

Introduction

The kinetics of functioning bacteriorhodopsin (bR) have been described by data from flash kinetic optical absorption (Lozier et al. 1975; Xie et al. 1987; Maurer et al. 1987), Raman spectroscopy (for review see Smith et al. 1985) and IR Fourier transform spectroscopies (Rothschild 1986). The photocycle has complex kinetics and is not clearly understood. Therefore, the application of new methods for investigating the kinetics of photoinduced processes in bacteriorhodopsin might be useful. Here we describe a method for measuring the kinetics of refractive index changes during the bR photocycle. The method appears to be useful for the investigation of a process which is practically unobservable in kinetic absorption spectroscopy.

Retinal – the prosthetic group of bacteriorhodopsin – has a transition dipole moment (transition from the ground to the first excited state) parallel to its geometric axis. On a microscopic level each individual molecule of chromoprotein absorbs light in an anisotropic manner owing to the direction of the transition dipole moment of its prosthetic group. Without special orientation procedures the purple membrane suspension (and hence the bacteriorhodopsin molecules) are randomly oriented and macroscopically the sample is isotropic. In the case of bR thin films on a glass substrate there is also no orientation in the film plane. Therefore, for the light crossing such a film perpendicular to the film plane the sample is isotropic.

Excitation of an isotropic medium by linearly polarized light leads to the development of anisotropic properties with the axis of anisotropy parallel to the excitation polarization. Testing such a sample with linearly polarized light enables the detection of differences when testing light polarization in front of and behind the sample.

The influence of the absorption anisotropy on the measured amplitudes in flash experiments with polarized light was described in detail by Nagle et al. (1983). However, anisotropy of absorption is not the only explanation for alterations in testing beam polarization. Another explanation for such alterations is changes in the refractive index. The influence of these two factors (absorption and refraction) is quite different: anisotropy of the refractive index cause elliptic polarization while anisotropy of the absorption coefficient cause a turn of the polarization axis (Savransky et al. 1987). It is possible to separate these effects and to obtain pure kinetics of the refractive index variations in the photochemical cycle of bacteriorhodopsin.

The experiments we describe deal with kinetic measurements of linear dichroism. The measurement of circular dichroism (CD) kinetics are also possible but require fine polarization techniques (Kliger and Lewis 1987). We believe that application of such a method can give new and interesting results, but in the case of our method we found no significant effect in CD.

Method

After excitation with a polarized light, an initially isotropic bR sample becames an anisotropic medium (Nagle et al. 1983). When rotation of the bR molecules (or rotation of the purple membrane fragments) is negligible, rotation of the transient dipole moment during the photocycle is also negligible (Czege et al. 1982). Thus, in our discussion we will suppose that the anisotropic axis of the bR sample does not change its orientation during the photocycle.

Here we will consider an experiment with the geometry shown in Fig. 1. Exciting and testing beams pass in the same direction (along the Z axis) and are linearly polarized. The angle between their polarizations is 45°. The testing beam is polarized along the Y axis and excitation polarization is shown by the dashed line in Fig. 1. The excitation polarization direction defines the induced anisotropy axis of the bR sample. We are interested in changes of the polarization of the testing beam after the sample and we will assume this change to be small so that only the linear term is present on expansion in series. For the sake of simplicity in all the following equations we will omit the amplitude term responsible for the isotropic absorption of the light and we will take into account only the first-order effects on the polarization state changes.

Polarization of the testing beam with unit intensity is defined by the system

$$\begin{cases} E_x = 0 \\ E_y = \sin(w\,t) \end{cases} \tag{1}$$

where E_x and E_y are the x and y components of the electric field respectively, w is the circular light frequency and t is time. Anisotropy of the refraction index of the sample gives elliptically polarized light after the sample

$$\begin{cases} E_x = f\cos(w\,t) \\ E_y = \sin(w\,t) \end{cases} \tag{2}$$
$$f = (n_o - n_e)\,l/2\lambda$$

where n_0 and n_e are refractive index for the ordinary and extraordinary beams, l is the sample thickness, and λ is the wavelength. Therefore, f is the retardation of the extraordinary component of the testing beam. The quantity f is directly proportional to the refractive index change during the bR photocycle and is fully determined by it and the constant parameters λ and l. Therefore, we will use this retardation as a measure of the refractive index change.

Anisotropy of the absorption changes cause a rotation of the light polarization axis by angle

$$a = (R_o - R_e)/(R_o + R_e) \tag{3}$$

where R_o and R_e are the absorption of the ordinary and extraordinary beams in the sample. Because of our assumptions $(R_o - R_e) \ll (R_o + R_e)$, it is possible to write equations for testing beam polarization

$$\begin{cases} E_x = f\cos(w\,t) + a\sin(w\,t) \\ E_y = \sin(w\,t)\ . \end{cases} \tag{4}$$

Equation (4) gives information about the change of the polarization of the testing beam after the sample. Term f defines the ellipticity and term a – rotation of the polarization. The simplest way to measure this polarization change is to measure intensity of the x component of the light. For this purpose we must put after the sample a polarizer crossed with the polarization of the testing beam before the sample and measure light intensity after it. The measured intensity will be

$$I = E\,E^* = (f)^2 + (a)^2 \tag{5}$$

so that it will be a mixture of both the refractive and absorption anisotropy effect. These type of experiments were carried out in our laboratory (Savransky et al. 1987). The signal defined by Eq. (5) is too complex for analysing the refractive index kinetics. Only wavelength with negligible contribution of absorption changes give "pure" information about the refractive index variation.

It should be possible to measure absorption coefficient changes during the bR photocycle and then subtract its effect from the composite signal given by Eq. (5). However, this is difficult in our instrument because of low accuracy for absolute measurements. Therefore, we chose another method to separate the two terms in Eq. (5).

If we add a quarter waveplate after the sample the polarization of the testing beam will change depending on the waveplate orientation. If angle v between the Y

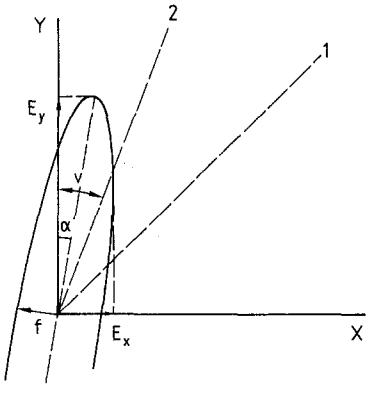

Fig. 1. A scheme of the experimental geometry. The testing beam is polarized along the Y axis, and the excitation beam is polarized as illustrated by the *dashed line 1*. The quarter waveplate axis is along the *dashed line 2* (the angle between its axis an the Y axis is v). Light exciting the system is elliptically polarized with ellipticity f and rotated by angle a

axis and the waveplate axis is small, then equations for the electric field of the beam after the waveplate are

$$\begin{cases} E_x = (f - v)\cos(w t) + (a + v)\sin(w t) \\ E_y = -\cos(w t)\,. \end{cases} \tag{6}$$

To derive these equations we transform system (4) to coordinates relative to the waveplate axis, add retardation $\pi/2$ for electric field component perpendicular to the waveplate axis, and transform the system to the inital coordinates.

As in the experiments discused above, the light intensity measured after the polarizer crossed with initial testing beam polarization will be

$$I = E\,E^* = (f - v)^2 + (a + v)^2\,. \tag{7}$$

Therefore, if we repeat measurements with a number of fixed angles v, it becomes possible to separate refractive (f) and absorption (a) effects by fitting the data with Eq. (7).

In the previous simple derivation we never took light absorption into account. More accurate analysis using only assumptions of smallness of angles (f, a, v) gives a modified equation

$$I(t, v) = T(t)\,((f(t) - v)^2 + (a(t) + v)^2), \tag{8}$$

where T is the coefficient responsible for the isotropic absorption changes. This is a second-order equation with one parameter (v) and three unknown values (T, f, a). Therefore we measure at least three kinetic curves $I(t, v)$ with different waveplate orientations v to calculate $f(t)$. Both $T(t)$ and $a(t)$ will show the usual absorption kinetics and may be used for checking the method itself and for control of the quality of fitting the data with Eq. (8).

Instrumentation and materials

The sample was prepared from a purple membrane suspension (a gift from Prof. R. Bogomolni) which was vacuum dried to form a thin film on a glass plate. The film was placed into quartz cuvette of 1 mm thickness filled with water, thus ensuring full hydration of the sample. The optical density of the film was about 0.5. The cuvette was placed into a thermostated cuvette holder. Experiments were carried out in the temperature range from 10° to 40 °C.

In our early experiments we used purple membrane suspensions, which are more optically homogenous than films. However, we found that rotational diffusion decreases the anisotropy and affects the measured signal. In suspensions the rotational diffusion time depends on the sample preparation procedure (e. g. sonication) and temperature. Its control requires additional experiments, so we decided to use purple membrane films.

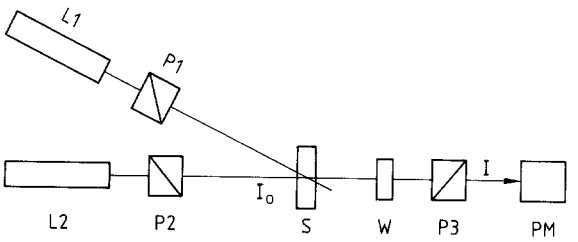

Fig. 2. A simplified optical scheme of the experimental setup. *L1* – excitation laser system ($\lambda = 532$ nm); *L2* – testing laser ($\lambda = 632.8$ nm); *P1, P2, P3* – polarizers; *W* – waveplates; *S* – sample; *PM* – photon multiplier; I_0 – testing beam intensity in front of the sample; *I* – testing beam intensity measured in our experiments

Figure 2 shows a simplified optical scheme of our experimental setup. We use the second harmonic of a passively *Q*-switched Nd:YAG laser (532 nm with 15 ns pulse duration and 2 mJ pulse energy) for excitation (*L 1*). A helium-neon laser (632.8 nm) is used for testing (*L 2*). The intensity of the testing beam is less than 1 mW/cm^2. We use a quasi-parallel scheme, so that the angle between the exciting and testing beams is only about 10°. Both the testing and exciting beams passed through polarizers (*P1, P2*) and the angle between their polarizations is about 45°. The sample (*S*) was attached to a rotatable holder so it could rotate around the testing beam propagation axis. After the sample the testing beam passed through the quarter waveplate (*W*) and polarizer (*P3*).

We used a 1 mm diameter diaphragm to select a relatively homogenous region of the sample so that polarization distortions after the non-excited sample (from spontaneous anisotropy of the purple membrane film plus anisotropy of glass) on the testing beam cross-section are minimised. These distortions are similar to the distortion of a one axis crystal and if we illuminate the sample with light polarized parallel to this axis there will be no polarization distortions of the beam. So the adjustment procedure is the following:

- only two polarizers (*P 2, P 3*) are placed in the testing beam path, and the last polarizer (*P 3*) is oriented so that no light passes;
- the sample is placed between the polarizers and adjusted by rotation of the sample holder to get the minimum transmittance of the testing beam through the system;
- the waveplate is placed between the sample and the last polarizer (*P 3*) and adjusted to get minimum transmittance of the testing beam through the system.

Before the measurement the spontaneous anisotropic axis of the sample was parallel to the testing beam polarization axis and we do not take into account the effect of this anisotropy.

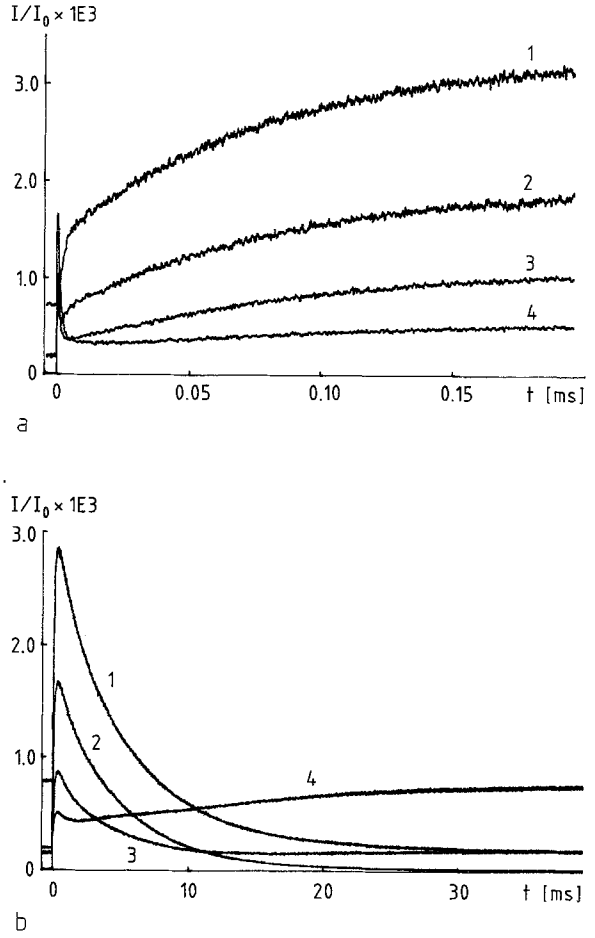

Fig. 3 a and b. Kinetic curves directly observed in experiments with a fully hydrated purple membrane at 20 °C, corresponding to the sum of effects from absorption and refraction anisotropy. I/I_0 is the ratio of the intensities of the measured testing beam to the testing beam before the sample. **a** and **b** represent fast and slow time bases respectively. Kinetic at quarter waveplate angle $v = 0.5°$ (curve 1), $v = 0°$ (curve 2), $v = -0.5°$ (curve 3) and $v = -1°$ (curve 4)

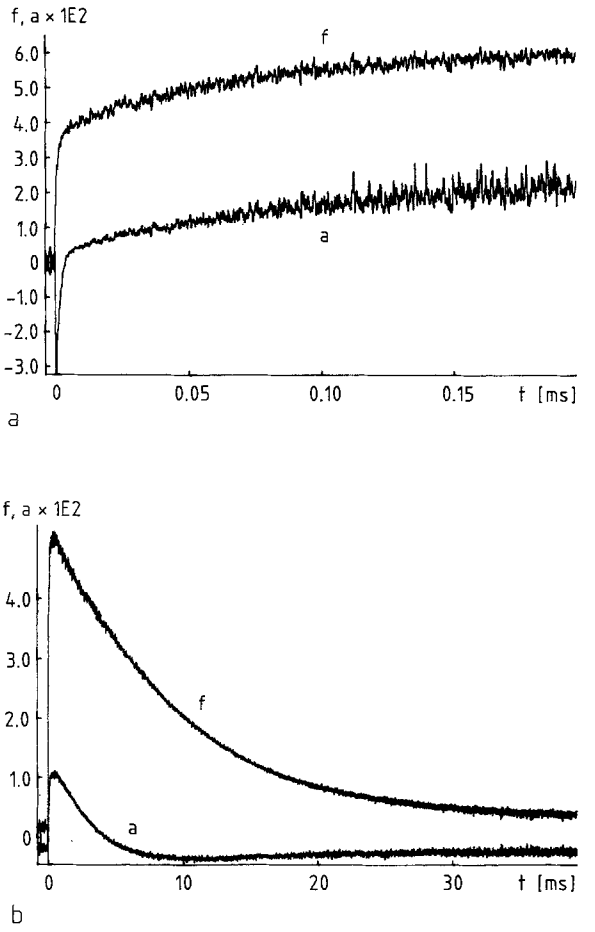

Fig. 4 a and b. Kinetics of the refractive index (f) and anisotropic absorption (a) at 633 nm and 20 °C. The curves were calculated from the data show in Fig. 3 by fitting to Eq. (8). **a** Fast time scale. **b** Slow time scale

In a similar experimental scheme Kliger and Lewis (1987) paid special attention to strain in the sample cuvette. Their cuvette was made from unstrained glass. Our use of the small diaphragm, laser testing beam source, and the described adjustment procedure allows us to use a common cuvette and the sample film.

The optical signal was measured by photomultiplier 100 (USSR) and recorded using a transient recorder, DL-922 (Data Lab, UK). The time resolution of our instrument is 100 ns. An Elektronica-60 (USSR) microcomputer was used for collecting data from the transient recorder and signal averaging with a repetition time of about 1 s. The microcomputer also controls both the excitation energy and testing beam intensity.

The same setup without polarizer *P 3* and waveplate is used for the actual kinetic absorption change measurements.

A set of curves with different waveplate angles v is fit to Eq. (8) using a linear least squares method to find coefficients $T(t), f(t)$ and $a(t)$ (transmittance, ellipticity and polarization rotation). A second program developed in our laboratory, based on a random search approach (Pronzato and Walter 1984), is used for multi-exponential fitting of the kinetic data.

Results and discussion

Figure 3 shows kinetic data obtained with a purple membrane film at 20 °C. We made separate measurements of the fast part (sampling time 50 ns, Fig. 3 a) and the slow part (sampling time 10 μs, Fig. 3 b) of the photocycle. The kinetics of the photocycle were measured with four different positions of the waveplate. Similar measurements were made at 10 °, 30 ° and 40 °C.

Kinetics of the refractive index $[f(t)]$ and anisotropic absorption $[a(t)]$ are shown in Fig. 4. These curves were obtained from the curves shown in Fig. 3

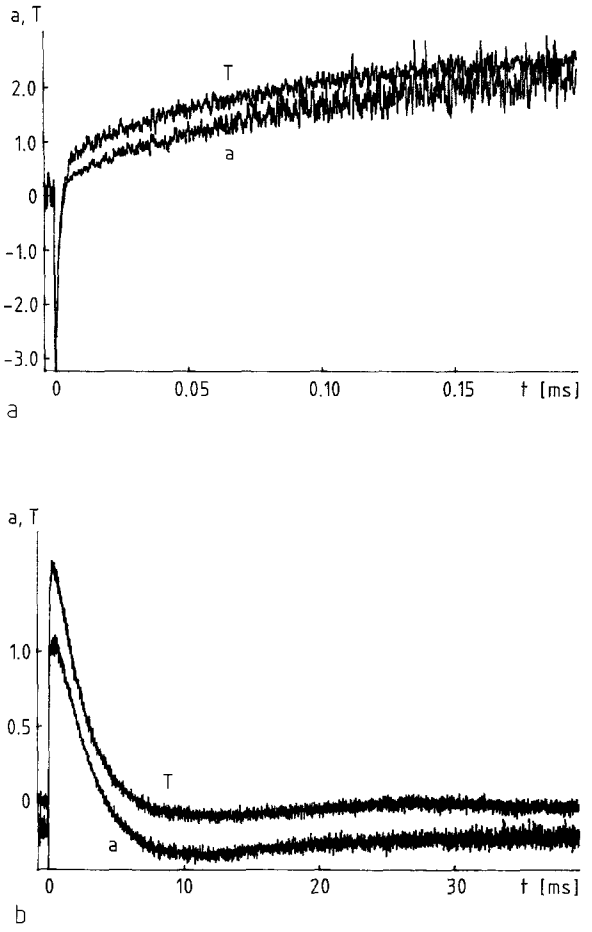

Fig. 5 a and b. Kinetics of the anisotropic absorption obtained using Eq. (8) (*a*) and absorption measured separately by standard the absorption kinetics method (*T*) at 633 nm and 20° in arbitrary units. The curves are slighty shifted on the vertical axis for clarity. **a** Fast time scale. **b** Slow time scale

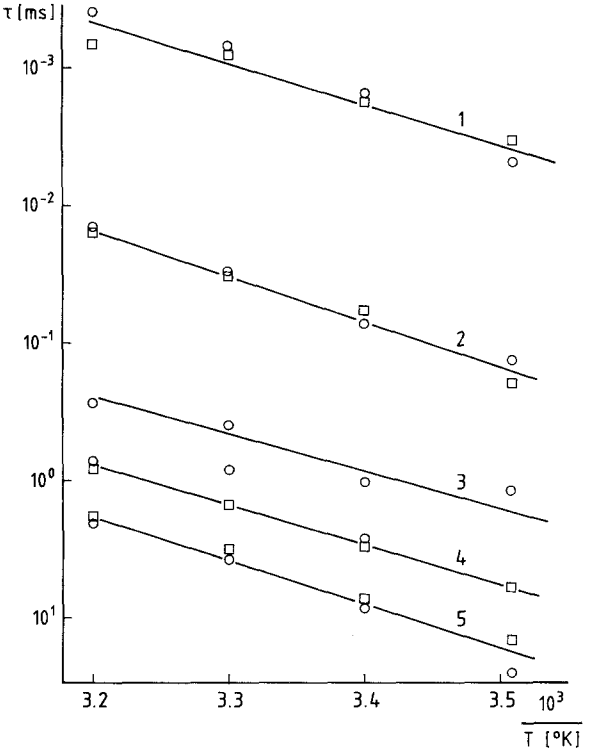

Fig. 6. Arrhenius plots of the time constants for the photochemical cycle of a purple membrane film in distilled water. The *circles* and the *squares* represent the time constants obtained by multi-exponential fitting of the refractive index and absorption coefficient kinetics, respectively

by using the least square approximation of Eq. (8). The absolute values of f and a are small, as we assumed in deriving Eq. (8). The only significant difference between the ansiotropic absorption and isotropic (absorption kinetics measured separately in our setup) was in the scaling factor (Fig. 5). We believe that this is good evidence of the applicability of our approach.

The absence of a difference between isotropic and anisotropic absorption kinetics means that there is no significant CD change during the bR photocycle or that the CD has kinetics similar to the absorption kinetics, since CD would also cause a rotation of linear polarized light.

We approximate the refractive and absorption kinetics by a sum of exponentials. Our multi-exponential fitting program calculates only time constants and amplitudes for a given number of exponentials, so we made calculations for different numbers of components and then compared the sum of the squares of the residuals and autocorrelation coefficients to make a decision as to the minimal number of exponentials needed for fitting. Except for the 10 °C data, a five exponential approximation is required for the refraction index kinetics. A four exponential approximation is enough for the 10 °C kinetics.

The refractive index kinetics differ greatly from the absorption kinetics at the wavelength of our experiment. In fact, the kinetics consist of a sum of exponentials with the same time constants but with different amplitudes. Figure 6 shows Arrhenius plots for the time constant we found for absorption (squares) and refractive index (circles) changes.

Refractive index kinetics in the fast part (Fig. 4 a) consist of an unresolved jump after the excitation pulse, corresponding to bR→K transitions, and two exponentials, corresponding to K→L and L→M transitions. In contrast to the absorption kinetics, the amplitude of the first component (fastest component in Fig. 6) is approximately half as large as the amplitude of the second component (L→M transition, curve 2 in Fig. 6). Therefore, the refractive index change gives more accurate data for the L→M transition at the 633 nm measuring wavelength. On the long time scale (Fig. 4 b) the most significated amplitude has the time constant usually associated with *M* intermediate decay signal (curve 5 in Fig. 6), and two more exponentials are extracted. One of them, usually associated

with 0 intermediate formation (curve 4 in Fig. 6), has a large amplitude in the absorption signal (at 633 nm) and a very small amplitude in refractive index kinetics. Its amplitude decreased with decreasing temperature and it disappeared at 10 °C. Another component is not usually found in flash-photolysis experiments (curve 3 in Fig. 6) and its amplitude had a maximum at 40 °C of about 30% of the refractive index signal. The amplitude decreases with decreasing temperature to about 10% at 10 °C.

The Arrhenius dependence for the four exponentials (curves 1, 2, 4, 5 in Fig. 6) are in agreement with the data reported from flash photolysis experiments of Xie et al. (1987) and Maurer et al. (1987). The fifth (curve 3) is present in the time domain where Xie et al. (1987) reported a component with very small amplitude and anomalous temperature dependence at pH 7. This component is absent in the data of Maurer et al. (1987). The component we found has an enthalpy of 40 ± 8 kJ/mol. The enthalpies of the other components are, using both absorption and refractive data, for curve $1-53 \pm 6$, $2-61 \pm 2.4$, $5-56 \pm 5$ and for curve 4 using only absorption data because of small refractive index amplitude -51 ± 1.4 kJ/mol. The absence in our results (as compared with the data of Xie et al. 1987) of two additional components is probably explained by the fact that our data is limited to only one recording wavelength.

Different factors may contribute to the variation of the refractive index. One of them is the appearance of a strong electric field of the order of 100 kV/cm on purple membranes during the photocycle due to proton pumping. Electric fields of this intensity affect electron clouds and can cause changes of the refractive index in a manner similar to this electrooptical effect in crystals. In electric measurements on bR membranes, a process with a lifetime of about 0.8 ms was observed (Fahr et al. 1981; Diomaev et al. 1984). Another reason is that the real part of the dielectric constant (square root of refractive index), is associated with the imaginary part of dielectric constant (responsible for the absorption) by spectral integral relation according to the Kramers-Kronig equation. Thus, a change in the absorption spectra in the UV, IR or visible range will cause a change in the refractive index. Thus the recorded refractive index kinetics may arise from of absorption variation in the UV, visible, and IR ranges.

Our experiments need to be extended to include other wavelengths and other pH values and salt concentration. Such data will give an opportunity to understand the nature of the refraction index changes during bR photocycle and may clarify details of the proton pumping mechanism.

Acknowledgements. The authors are grateful to A. K. Diomaev and R. H. Lozier for useful discussions and assistance in some of the experiments, to I. Chizov for preparation of the purple membrane film, and to Drs. D. Klinger, J. Lewis and C. Einterz for useful comments on a preliminary draft of the manuscript.

References

Czege J, Der A, Zimanyi L, Keszthelyi L (1982) Restriction of motion of protein side chains during the photocycle of bacteriorhodopsin. Proc Natl Acad Sci USA 79:7273–7277

Diomaev AK, Savransky VV, Vasiljev GV, Vladimirova RR, Malina ZA (1984) On kinetics of occurrence of photoinduced potential difference in a model system containing bacteriorhodopsin. Biofizika (USSR) 19:389–392

Fahr A, Läuger P, Bamberg E (1981) Photocurrent kinetics of purple-membrane sheets bound to planar bilayer membranes. J Membr Biol 60:51–62

Kliger DS, Lewis JW (1987) Recent advances in time resolved circular dichroism spectroscopy. Rev Chem Intermediates 8:367–398

Lozier RH, Bogomolni RA, Stoeckenius W (1975) Bacteriorhodopsin: a light-driven proton pump in *Halobacterium halobium*. Biophys J 15:955–962

Maurer R, Vogel J, Schneider S (1987) Analysis of flash photolysis data by a global fit with multi-exponentials. Photochem Photobiol 46:247–262

Nagle JF, Bhattacharjee SM, Parodi LA, Lozier RH (1983) Effect of photoselection upon saturation and dichroic ratio in flash experiments upon effectively immobilized systems. Photochem Photobiol 38:331–339

Pronzato L, Walter E (1984) A general-purpose global optimizer: Implementation and applications. Math Comput Simul 26:412–422

Rothschild KJ (1986) Fourier transform infrared studies of an active photon transport pump. In: Packer L (ed) Methods in enzymology, vol 127. Academic Press, New York, pp 343–353

Savransky VV, Tkachenko NV, Chukharev VI (1987) Refraction index changes in bacteriorhodopsin photocycle. Biol Membr (USSR) 4 (5):479–485

Smith SO, Lugtenburg J, Mathies R (1985) Determination of retinal chromophore structure in bacteriorhodopsin with resonance Raman spectroscopy. J Membr Biol 85:95–109

Xie AH, Nagle JF, Lozier RH (1987) Flash spectroscopy of purple membrane. Biophys J 51:627–635